Max-Planck-Institut für extraterrestrische Physik
Giessenbachstrasse
85748 Garching
Germany

Michael Freyberg
Tel: +49–89–30000–3849
Fax: +49–89–30000–3569
Email: mjf@mpe.mpg.de

eROSITA Commissioning and In-Orbit Calibration Plan

Design and Strategy

eRO-MPE-PL-55-01_01

M.J. Freyberg, K. Dennerl

Max-Planck-Institut für extraterrestrische Physik

Version 0.1 30-06-2012, 0.2 21-07-2012, 0.3 31-08-2012, 0.4 25-09-2012, 0.5 28-09-2012, 0.6 02-10-2012, 1.0 11-10-2012

Abstract

This draft describes the on-ground calibration strategy and the relation to in-orbit commissioning and calibration observations. A tentative list of targets (more target classes rather than individual objects due to unknown launch date and thus unknown visibility windows) is shown with equatorial coordinates, galactic longitude (for data rights), and ecliptic latitude (for visibility).
Updates on the target list will be given (until a major revision of the paper) only at
`http://www.mpe.mpg.de/~mjf/CalPV/`

Change Record

Issue	Date	Description of Change	Affected Pages
(0.1)	2012-06-30	New document, first proposal	All
(0.2)	2012-07-21	Comments on targets	All
(0.3)	2012-08-31	Multi-wavelength information into web page	
(0.4)	2012-09-25	eROSITA document format	All
(0.5)	2012-09-28	added galactic and ecliptic coordinates	
(0.6)	2012-10-02	added few more targets, Sun angle $90° \pm 20°$	
1 (1.0)	2012-10-11	more targets, galactic, ecliptic coordinates	
		Web page with multi-wavelength info (etc)	

Distribution List

Organisation	Name	Organisation	Name
MPE	eRO document server		
eRO	MJF FTP server		

Approvals

Function	Name	Date	Signature
Author	M. Freyberg	2012-10-11	N/A
Product Assurance			N/A
Project Manager			N/A
System Engineer			N/A
Principal Investigator			N/A

Contents

1 INTRODUCTION

1.1 Applicable and Reference Documents

1.1.1 Applicable Documents

1.1.2 Reference Documents

RD1 : D. Lumb, "EPIC In-Flight Calibration Program",
XMM-PS-TN-023, Issue 1 (1997-05-30)

RD2 : Ph. Gondoin, C. Erd, D. Lumb, R. Much, "In-orbit XMM Calibration Plan",
XMM-PS-GM-19 (CAL-PL-0002-1-1), Issue 1.1 (1999-03-03)

RD3 : M.J. Freyberg, K. Dennerl,
"eROSITA in-orbit calibration strategy and plan: from the ground to the science",
Proc. SPIE **8448**, 84480Y 1–10 (2012); doi:10.1117/12.927083
`http://proceedings.spiedigitallibrary.org/proceeding.aspx?articleid=1359142`
`http://www.mpe.mpg.de/~mjf/freyberg_spie_8448_33_final.pdf`

RD4 : M.J. Freyberg, K. Dennerl,
"On the eROSITA in-orbit calibration strategy and plan",
Poster presented at eROSITA/ART-XC/SRG conference, Kazan, Sept.2012;
`http://hea.iki.rssi.ru/kazan2012/Presentations/df6d096a87199ddfd41afcaa74725eb3.pdf`
`http://www.mpe.mpg.de/~mjf/ero_kzn_cpv_expand_a0.pdf`

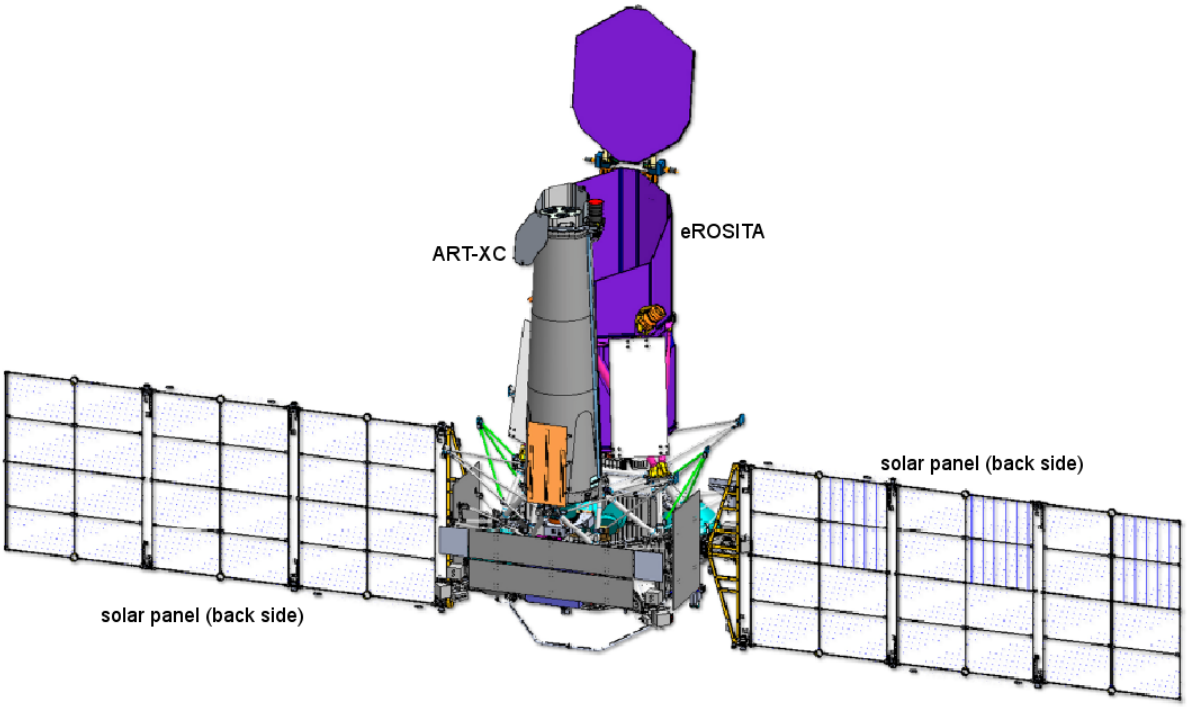

Figure 1: The Russian Spectrum-Roentgen-Gamma (SRG) satellite with the German soft X-ray telescope *eROSITA* (in purple, with front cover opened toward the Sun) and the Russian hard X-ray instrument ART-XC (in grey), with deployed solar panels, mounted onto the Navigator platform (adapted from Pavlinsky et al., 2011)

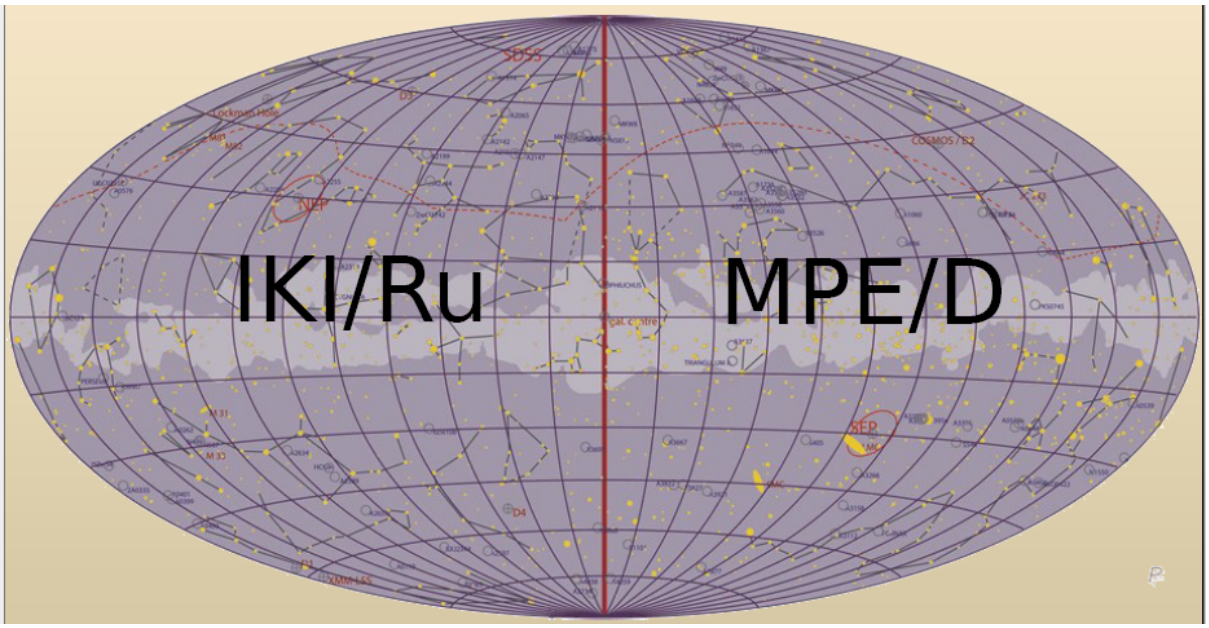

Figure 2: Data rights for the *eROSITA* sky in galactic coordinates (image courtesy P.Friedrich & P.Predehl, MPE).

2 eROSITA MISSION SCENARIO

SRG is expected to be launched from Baikonur in 2014 with a Zenit/Fregat rocket. After about 100 days it will be reach a halo orbit around the libration point L2 (1.5 million km away from Earth). Figure 1 shows the SRG satellite with payload installed on the Navigator platform. The nominal lifetime is 7 years, with a 3-year pointed observation programme following the survey phase. Data will be transmitted to ground via the X band ($\sim 7.5\,$GHz) with a telemetry rate of 512 kb/s during ground contacts.

The *eROSITA* sky will be divided into two halves in galactic coordinates along a great circle over the galactic poles through the galactic center[1]. MPE owns the data rights for the "western" part ($l = 180° - 360°$) while the Russian partner institute IKI owns the "eastern" part ($l = 0° - 180°$). A strip of 1° width centered on the dividing line is owned by both parties simultaneously. Each partner has access to all sky data, but scientific exploitation is limited to the respective hemisphere. Figure 2 illustrates the sky division.

3 eROSITA INSTRUMENTATION

3.1 Mirror module

The *eROSITA* instrumentation aboard SRG will consist of 7 mirror modules of 54 shells each, equipped with 7 CCD cameras as focal plane instruments, looking in parallel to the sky. The main scientific goal (quest for "dark energy", e.g. by the detection and analysis of clusters of galaxies) requires especially a good spatial resolution, i.e. HEW < 15" at 1.5 keV and < 20" at 8 keV, on-axis for a full mirror module. Mandrels from the ABRIXAS programme (inner shells, #28 through #54) are used together with new mandrels (outer shells, #1 through #27) to replicate gold-coated nickel shells via electro-forming. Each of the mirror modules is accompanied by an X-ray baffle to suppress stray light from sources outside the FOV (from single reflections off the hyperboloid). The mirror modules will be

[1]More precisely speaking, the dividing line passes through Sgr A, $l = 359.9443°$, $b = -0.0462°$.

device	process	signal	characteristic properties	
telescope	reflection (scattering)	*photon [eV]*	effective area (E,φ) point spread function (E,φ) field of view (FOV) boresight	collecting area, reflectivity, vignetting mirror quality focal length, detector geometry, plate scale alignment
filter	absorption		transmission (E) contamination (E,t)	filter thickness, spatial homogeneity temporal behaviour
CCD	charge release	*charge [e⁻]*	charge splitting low energy threshold	**patterns** (singles, doubles, triples, quadruples, invalid..)
			contaminating effects	**pile-up** (single pixel, pattern) **photon background** (fluorescence, optical loading)
			quantum efficiency (QE) energy resolution (ΔE)	**particle induced background** (soft protons, MIPs) **detector induced background** (noise, bright pixels)
	charge transfer		charge transfer loss (CTI) pattern migration	**trap saturation** due to photons and particles **charge transfer noise** **threshold induced charge loss** reemission, charge diffusion, charge splitting
	charge readout	*pulse height amplitude [adu]*	readout noise amplification ('gain')	non-linear gain, also dependence of the "apparent" gain on threshold(!) dependence on energy, temperature, time
on-board data processor	signal processing	*event [bit]*	energy offsets (offset map) common mode correction signal extraction MIP suppression	**restrictions likely due to limitations in on-board computing power and telemetry** (low energy threshold, MIPS..)

Figure 3: The way of photons from the telescope through the camera to the data acquisition system.

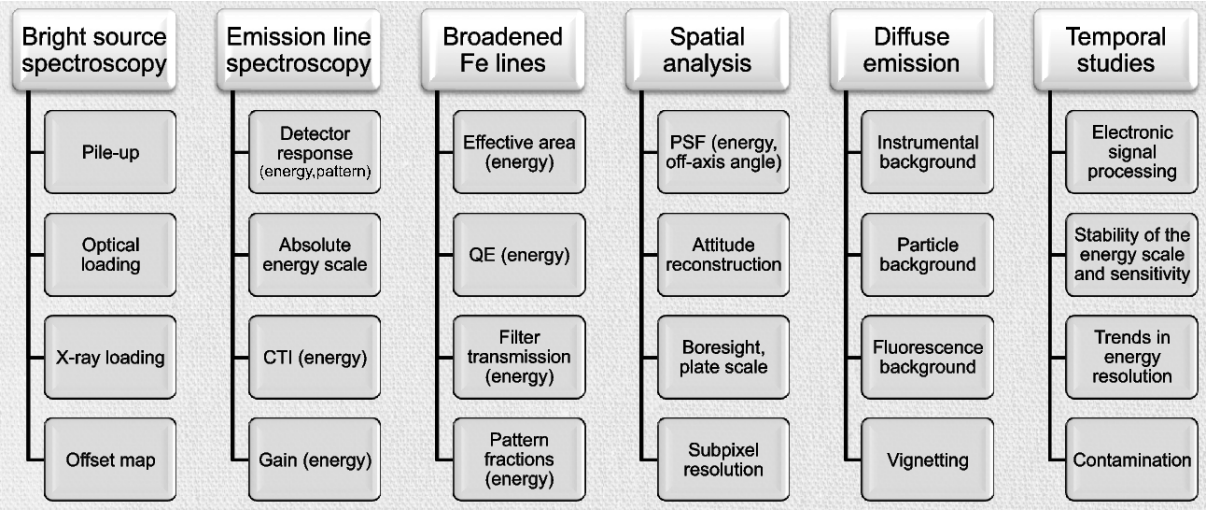

Figure 4: Science subjects and their relation to and relevance for calibration subjects.

individually calibrated on-ground, first without and then with the mounted X-ray baffle, and with its own CCD camera. The conversion from photons to bits is shown in Fig.3.

3.2 Frame-store pnCCD camera

The *eROSITA* focal plane cameras are based on newly developed frame-store pnCCDs. They provide 384×384 pixels of $75\,\mu$m size ($28.8 \times 28.8\,\mathrm{mm}^2$), corresponding to a spatial resolution of about $10''$ which can be improved using sub-pixel resolution techniques. As a backside-illuminated device it is intrinsically radiation-hard, it is operated at about $-90°$ C. With a silicon thickness of $450\,\mu$m they have an excellent quantum efficiency (QE) at higher energies. At lowest energies the QE is limited by the optical light blocking

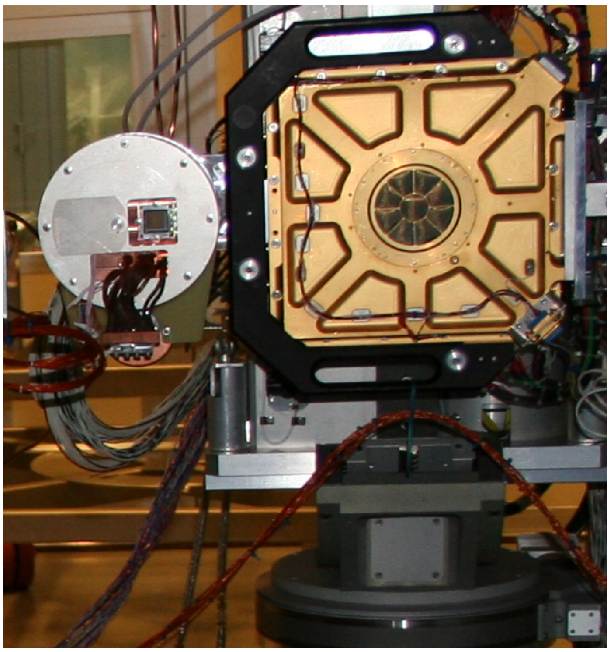
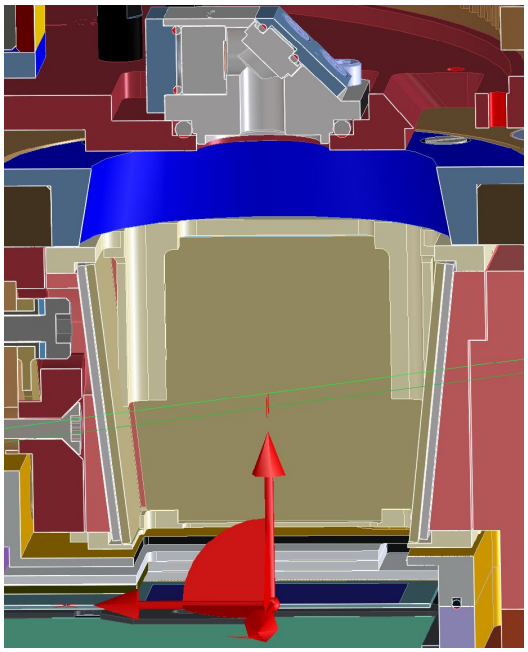

Figure 5: Left: Focal plane instrumentation at PANTER, (from left to right:) pnCCD camera TRoPIC (small, left), proportional counter PSPC (large, right). Right (image courtesy B.Mican, MPE): cross-section of *eROSITA* filter wheel with internal calibration source based on Fe-55 (top-left) and Al/Ti target (top) and CCD at the bottom.

filter. Two batches of flight CCDs have been produced, one with on-chip filter of 200 nm aluminum on Si_3N_4 and SiO_2, and the other without on-chip filter. The latter need an external light blocking filter as optical light shall be suppressed by a factor of the order 10^{-6} to prevent extraneous events caused by optical photons. Each camera is equipped with a filter wheel with 4 positions: one "Closed" (4 mm aluminum), one "CalClosed" (with internal calibration source) one "Open" and another one with an external light blocking filter (for CCDs without on-chip filter, for the others an additional external filter were possible). The baseline for the external filter is a 100 nm aluminum layer on a 200 nm polyimide foil.

3.3 Internal calibration source

The *eROSITA* internal calibration source (based on Fe-55) will be mounted on the filter wheel on one of the four "stop" positions and can be turned in and out of the field-of-view. The spectrum will mainly consist of Mn-Kα and Mn-Kβ (5.89 and 6.49 keV) lines following the radioactive decay of Fe-55 (electron capture) and fluorescent Al-K (1.49 keV) and Ti-Kα (4.51 keV) and Ti-Kβ (4.93 keV) from a target plate. The target is hit by the Mn-K X-rays at an angle of about 45° and X-rays are registered by the CCD at further 45° angle. The distance of the CCD from the exit of the calibration source is about 53 mm, from the target about 10 mm more (see Fig.5 right).

3.4 Auxiliary devices

A star-tracker and a sun-sensor are mounted onto the *eROSITA* telescope. This ensures that effects of the platform do not influence attitude reconstruction of *eROSITA* (data belong to the spacecraft).

4 CALIBRATION METHODS

4.1 Measurements on-ground

4.1.1 Facilities

X-ray CCD cameras need to be operated at low energies for best performance, typically $-90°$ C and therefore need high vacuum of the order of 10^{-5} mbar or better. MPE operates two X-ray test facilities, one with a 6 m vacuum chamber (PUMA, in Garching) and one long beam-line facility (PANTER, in Neuried) with a 12 m vacuum chamber and 120 m vacuum tube and various X-ray sources at the other end. The latter length is motivated by the fact that in mirror calibration one needs to reproduce a practically parallel incident beam as is the case for celestial X-ray sources, by putting calibration X-ray sources as point-like and as far away as possible to minimize the beam divergence. At PANTER the focal plane instrumentation (see Fig.5 left) for *eROSITA* calibration consists of the PSPC and TRoPIC (plus the corresponding calibrated *eROSITA* camera).

The position-sensitive proportional counter (PSPC) provides moderate spectral (40% at 0.93 keV) and spatial (280 μm) resolution, but it is well-suited for measuring effective areas as it is an exact photon counting device and not affected, e.g., by pile-up (two photons hitting the same or neighboring pixels in the same read-out cycle) present in CCD devices when exposed to high fluxes. The wide field-of-view of 80 mm diameter is useful for alignment procedures as well as for the analysis of mirror scattering.

TRoPIC is an *eROSITA* prototype camera operating in frame-store mode and was specially developed for calibration measurements at PANTER, for *eROSITA* and high-energy missions like SIMBOL-X. With a pixel size of 75 μm $\times$ 75 μm, a cycle time of about 50 ms, an out-of-time event fraction of 0.2%, and a 256 $\times$ 256 pixel FOV (19.2 mm $\times$ 19.2 mm) it is well suited for PSF measurements and high-resolution imaging. Moreover, various gain levels are available to optimize the amplification according to the incident X-ray spectrum.

Typically, detector calibration will take place at PUMA (no need for long beam-line) and mirror calibration at PANTER. The main calibration measurements at PUMA will cover the energy response with charge transfer inefficiency (CTI), gain, pattern fractions, and quantum efficiency (including the filter transmission), as function of incident energy.. At PANTER, the main calibration goals will be with respect to the mirror properties: effective area and point spread function (PSF) as function of off-axis angle and incident energy, this includes also the performance of the X-ray baffle which will formally be incorporated into the PSF.

The ground calibration of the detector requires several types of measurements. These measurements should all satisfy the following minimum requirements: intensity shall be as high as possible, but avoiding (pattern) pile-up; the full CCD should be homogeneously irradiated in a flat-field-like mode; distinct emission lines must be present in the incident -ray spectrum; The X-ray range shall cover the nominal energy range. Depending on the individual calibration goal, additional requirements are necessary to determine the relevant parameters. An overview is given in the table below. The scope of the various calibration measurements is summarized in the following sections, the relation to the science is shown in Fig.4.

4.1.2 Charge transfer inefficiency

The determination of the CTI is necessary for the correction of the measured energy of a registered photon, since part of the charge (electron cloud), produced by the photon, gets lost in traps, caused by contamination of the silicon basic material with, e.g., titanium. For this determination, flat-field measurements are necessary at several X-ray lines. In

Table 1: Purpose of calibration measurements with requirements.

Purpose	spectral quality	spatial quality	statistical quality	calibrated flux	remarks
CTI	low	low	very high	no	0.18, 0.28, 0.93, 1.49, 4.51, 5.89, 8.04 keV
Gain	low	low	high	no	
Detector response	very high	low	high	no	
Pattern fractions	high	low	low	no	
Quantum efficiency	high	low	low	yes	
... at spectral edges	very high	low	low	yes	
Spatial homogeneity	low	very high	high	no	
Offset and noise map	n.a.	n.a.	n.a.	n.a.	
"Closed" background	n.a.	n.a.	n.a.	n.a.	minimize
Spatial resolution	no	low	high	no	verification, pinhole mask
Timing	no	low	high	no	only verification

addition, the internal calibration source (see Fig.5 right) will also be used for the CTI determination.

4.1.3 Gain

The gain of each read-out channel of each of the 7 cameras is needed to determine the energy of a registered photon. The same calibration measurements as in Sect.4.1.2 can be used for the determination of the gain, and thus no extra calibration time is needed.

4.1.4 Spectral resolution and the redistribution matrix

The spectral resolution and the redistribution matrix of each detector is necessary for fitting measured spectra of celestial objects to possible X-ray source models. Measurements will need to be performed with spectrally clean X-ray lines, preferably produced with an X-ray monochromator, especially around the Si-K and O-K edges.

4.1.5 Pattern fractions

The electron cloud produced by a registered photon via the photo-effect electron, is for more than half of the absorbed photons spread over more than one pixel. Hence a photon can deposit its charge in one pixel (single-), two pixels (double-), three pixels (triple-) or four pixels (quadruple-event). The energy distribution of single and split events is dependent on the energy of the photon and the low energy threshold(s). The determination of the pattern fractions (of singles, doubles, triples, and quadruples) as a function of the incident X-ray energy is necessary for reconstructing the incident photon flux. The fractions are also related to the ability to perform a spatial analysis using sub-pixel resolution. Measurements performed according to Sec.4.1.4 can be re-used here.

4.1.6 Quantum efficiency (QE)

The quantum efficiency (QE) of each detector is essential to determine the absolute flux of celestial objects. The QE includes not only the CCD itself but also on-chip and/or external (light-blocking) filters. For all QE measurements, an X-ray source with calibrated flux, or an absolutely calibrated flux monitor, is mandatory. An absolute accuracy of 10% is envisaged.

4.1.7 Spatial homogeneity

The spatial homogeneity of the QE of each detector (CCD plus filters) is needed to "flat-field" the exposure maps, necessary for deriving the correct X-ray flux. The calibration measurements for the CTI and gain determination can be used for this, provided that the X-ray beam is sufficiently homogeneous.

4.1.8 Offset and noise maps

The offset maps are necessary for the read-out of registered events and have to be calculated before the measurements. They are, together with the noise maps, important diagnostic tools to monitor the health of the detector. At the same time, they are used to determine the number of dead/hot pixels.

4.1.9 Determination of the "Closed" background

The knowledge of the detector background is essential for many measurements, in particular at the lowest energies and for low-surface brightness (faint extended) objects.

4.1.10 Spatial resolution

The spatial resolution of each detector will be verified at several X-ray energies. Although the spatial resolution is given by the pixel size of the CCD, a sub-pixel resolution can be obtained, utilizing the fact that more than 50% of the photons produce split events. In this case, the pattern type and the (energy dependent) charge fraction in the pixels can be used for an improved determination of the position where the photon was absorbed.

4.1.11 Relative and absolute timing resolution

The (relative and absolute) timing resolution is necessary to measure time profiles of celestial sources. Resolution is given by the frame-time of the CCD read-out ($\sim 50\,\mathrm{ms}$). The time stamping accuracy (camera plus spacecraft) determines the absolute timing resolution. Relative accuracies can be obtained in functional tests of *eROSITA* on-ground, absolute accuracies are only available on a fully integrated level (including ground station effects).

4.1.12 Point spread function (PSF)

The knowledge of the energy dependent point spread function (PSF) is essential to determine the absolute flux of celestial objects. Width and shape determine the encircled energy fraction within a certain radius. Different roll angles and off-axis angles are necessary to determine the shape of the PSF, which is a function of the off-axis angle and which can vary with the roll angle due to the spider wheel and imperfections of the mirror shells. Since on-ground the X-ray source is at a finite distance to the mirror, a "Glücksrad" will be used for the measurements. In this set-up only a small area of the mirror entrance (hence small divergence) is illuminated by the X-rays, which is set to the desired incidence angle. These apertures can be changed in radius and azimuth, and thus unbiased characterization of the whole mirror module is possible. One telescope system will be calibrated in larger detail, the others with a reduced calibration program. High spatial resolution without pile-up (see below) is required.

4.1.13 Pile-up

Pile-up occurs if more than one photon is registered within one readout frame in a specific pixel (normal pile-up) or by neighboring pixels (pattern pile-up). This effect depends strongly on the count rate. It is essential to calibrate the pile-up effect at different count rates in order to determine the absolute flux of celestial objects. In-orbit pile-up in pointed observations can be reduced by setting a source off-axis to utilize the general spatial broadening of the PSF with increasing off-axis angle. In the scanning survey phase pile-up effects may be time-variable during a pass through the FOV.

4.1.14 Effective area

The knowledge of the energy dependent effective area is essential to determine the absolute flux of celestial objects. Different roll angles and off-axis angles are necessary to determine the vignetting, essential for the "flat-fielding". Due to the finite source distance on-ground, a "Glücksrad" will be used (see Sect.4.1.12). Spatial resolution of the camera involved in the effective area calibration is unimportant, therefore the PSPC as photon counting device without pile-up is here superior to TRoPIC (or other CCD cameras).

4.1.15 Stray-light

Sources outside the FOV can produce a "background" in the FOV ($\sim 30'$ radius) by single reflections off the hyperboloid part of the mirror shells. The relevant off-axis angle range for *eROSITA* is of the order of $30' - 190'$. In pointed observations for point sources these single reflections occur as arc-like features; for significantly extended objects or for survey scans across the sky these effects can only be recognized as additional background. This stray-light can very efficiently (but not completely) be reduced with the X-ray baffle.

4.1.16 Focal length

The focal length of all mirror modules will be determined on-ground with an accuracy of ~ 0.1 mm. The precise knowledge of the focal length is essential to integrate the detector at the optimal spot. Finite source distance effects (shift of focal image location) will be taken into account. No in-orbit measurements possible related to focal length except for PSF comparison.

4.2 Measurement phases in-orbit

4.2.1 Motivation

Changes of the on-ground calibration performed at PUMA and PANTER are expected after launch. In particular, radiation damage will increase the charge transfer inefficiency. Furthermore, effects due to the launch cannot be excluded *a priori*. Later, contamination effects or micrometeoroid impacts should be looked at. Finally, yet unknown effects could require a re-calibration of parts or properties of the instrumentation, such as integrity of optical light blocking filters, integrity of mirror shells and X-ray baffle, mirror module orientation (with respect to star tracker and other modules), performance like PSF or effective area, etc.

4.2.2 Launch

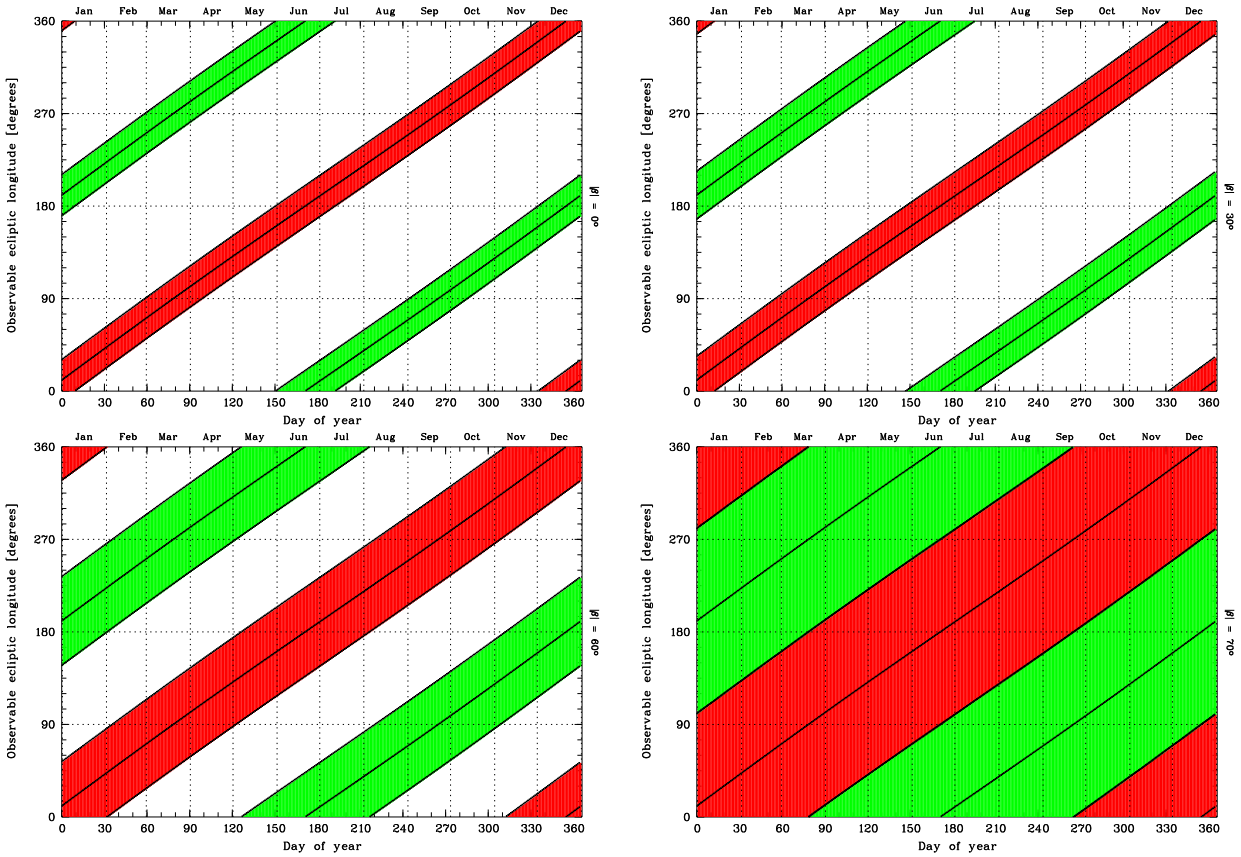

Figure 6: Observability of celestial targets as function of ecliptic longitude during 2015 from *eROSITA* with an assumed maximum allowed solar elongation angle of $90° \pm 20°$ for several ecliptic latitudes: $|\beta| = 0°$ (top left), $|\beta| = 30°$ (top right), $|\beta| = 60°$ (bottom left), $|\beta| = 70°$ (bottom right). Red and green areas indicate the different halves of the ecliptic great circles. This information is an important input for the selection and scheduling of celestial calibration targets. Targets with $|\beta| > 70°$ can be observed at any time.

After successful functional end-to-end test of *eROSITA*, transport to Russia, integration and check-out with SRG, the launch (scheduled for 2014) will bring *eROSITA* out of physical contact and hardware cannot be serviced anymore (especially not at L2), only software updates are possible. All further actions will have to be performed remote controlled, either online during ground contacts or routinely via time-lines (long-term, mid-term, short-term) and time-tagged commands. After launch, substitution heaters will be switched on, and once the spacecraft is in a stable configuration the front cover will be opened (see Fig.1). Check-out of the instrumentation can begin while outgassing continues for about 2 weeks.

4.2.3 Commissioning

During the transfer phase to L2 switch-on of the cameras will take place one after another. After initial health checks the cameras will be operated with “Closed” and “CalClosed” filter wheel positions. Several instrument parameters will be fine-tuned such as lower event thresholds (trigger threshold and split threshold) or parameters related to the on-board rejection of minimum ionizing particles (MIPs). After turning the filter wheel into “Open” (for CCDs with on-chip filter) or “Filter” (external filter for CCDs without on-chip filter) the filter integrity can be checked by the response to optical light, e.g., of stellar clusters. The actual celestial targets depend on target visibility, and thus on the actual launch date and on the ecliptic latitude of the celestial target (see Sect.4.3). Therefore target close to the ecliptic poles are preferred as these can be observed at any time (see Fig.6).

For telemetry reasons, also pair-wise observations of a celestial target could be considered (with, e.g., the other cameras performing background observations).

4.2.4 Calibration

Several calibration parameters could only be determined approximately such as the PSF and vignetting and absolute timing. Therefore celestial targets dedicated for a specific calibration subject have to be chosen, (only celestial sources are available for mirrors, no internal source illuminates the mirrors). The sources should be X-ray bright (statistics) but not too bright (pile-up, telemetry). Also they should be optically not too bright (depending on filter, note that the optical PSF differs from the X-ray PSF). The actual calibration parameters can be derived from any suited celestial target. Proprietary rights are to be respected, i.e., celestial targets from the calibration phase shall only scientifically be exploited within the lead of the respective "hemisphere institutes" (see Fig.2). Simultaneous observations of the 7 *eROSITA* cameras are an important tool for cross-calibrating the instruments. If, e.g., XMM-Newton is still operational at that period, a dedicated cross-calibration campaign with EPIC is desired. ART-XC is looking in parallel to *eROSITA* and thus generically simultaneous data for cross-calibration are obtained.

4.2.5 Performance verification

After the calibration a phase with performance verification is planned. This could include a mini-survey (several great-circle scans across the ecliptic poles), and would be useful to determine spacecraft parameters (e.g., time delays of star tracker relative to CCD cameras) or single-reflection straylight effects, e.g., passing close ($\sim 30' - 190'$) to Sco X-1 (also possible by a series of dedicated mosaic pointings). As mentioned above, target visibility determines the selection and sequence of observed celestial targets (e.g., Sco X-1 in March or September).

4.2.6 Monitoring

To verify presumably variable calibration parameters such as CTI or low-energy performance non-variable sources on times scales of the *eROSITA* lifetime are preferred for monitoring, such as the internal calibration source (practically only the brightness is changing but not the spectrum) or supernova remnants or isolated neutron stars (these targets should be scheduled regularly like every 6 months after each all-sky survey or every 12 months and restart of the survey phase without gap afterwards).

4.3 Celestial targets and visibility

Several important celestial targets are only visible for a short period, and thus a flexible programme should be set up to observe (as many as possible of) these targets (see Fig.6). So the order of the calibration subjects will have to be adjusted according to the actual launch date. The various calibration items mentioned in Sect.4.1 require different targets. These include:

1. filter integrity (on-chip, external): bright diffuse optical source, e.g. Omega Cen;
2. contamination: on CCD or mirror: soft sources, e.g. isolated neutron stars ("Magnificent Seven") or white dwarfs: RX J1856.5-3754 (INS) or GD 153 (WD);
3. PSF: point-like sources, should not be too bright on-axis, may be brighter off-axis;

4. effective area and vignetting: non-variable source, maybe slightly extended or very extended (e.g., Coma cluster);
5. gain (energy scale): featureless source spectrum (e.g. power-law): use instrumental edges, e.g., 3C 273, moderately line-rich spectrum: e.g., SNR: 1E 0102-72, N132D;
6. CTI, event pattern: Fe-55 ("CalClosed" filter wheel position), or Vela SNR (O VII, O VIII).;
7. spectral response function: width, shelf (partial events): highly absorbed sources, low intrinsic continuum;
8. plate scale, boresight: field with many sources with known locations: LMC or stellar clusters: e.g., NGC 2516, NGC 6475 (M 7), NGC 752, Hyades;
9. attitude reconstruction and relative timing of cameras and star tracker: slews ("mini-survey") over stellar clusters, pulsars, etc.;
10. stray light (X-ray baffle relative to mirror): scan or mosaic close to Sco X-1 or Crab (out-of-FOV: $30' - 190'$ off-axis);
11. background: filter wheel in closed position (4 mm Al), CCD corners;
12. relative timing of cameras: pulsar with period $P = 0.5 - 10$ s.

Monitoring using the internal calibration source shall be performed with one camera at a time to make the sky coverage homogeneous, and also to reduce the data amount (calibration source is brighter than sky). It is expected that at the beginning about 5 minutes "CalClosed" are sufficient, with decaying intensity later longer exposures are needed. With a 4 h revolution a segment of about 8° would be affected. These monitoring periods will be incorporated into the general "survey efficiency" figure. This means for one run (i.e., 7 cameras) the survey exposure for about 1/6 of a revolution (60°) is reduced by a factor 6/7. These periods would be located on both hemispheres, preferentially not at regions of lowest exposure.

5 APPENDIX: List of targets

5.1 Target positioning

If possible, no star brighter than $m_V < 4$ shall be in the FOV of a calibration target in pointed observation mode. This limit shall be refined after filter selection and calibration.

5.2 Target sequence

The sequence of observations is mainly driven by the visibility of the individual targets. As far as contamination is concerned, bright UV source shall be observed later in the calibration phase to avoid possible polymerization. In this context it is suggested to switch on the cameras with external filter first as these are less sensitive to external contamination (and leave the others with filter wheel in "Closed" position).

Moreover, the commissioning and calibration of ART-XC (looking in parallel to *eROSITA*) also influences the *eROSITA* programme.

5.3 Targets for commissioning

The LMC is preferred as it is always visible. As the cameras will be switched on one by one, the LMC would provide the same field for all the cameras (until all cameras are operational). For the first camera 1 week is needed, the following cameras could be switched on with a rate of 2 per week (i.e., total time 4 weeks). Data right details for commissioning phase have to be clarified (default is general survey policy).

5.4 Targets for calibration

It is proposed that for calibration each Working Group provides a list of suited targets and/or black-listed targets. Data right details for calibration phase have to be clarified (default is general survey policy).

Furthermore, a "Mini-Survey" as early as possible is suggested similar to ROSAT. This could help to identify any time delays between the various instruments (*eROSITA*, star tracker, etc.) and also to clarify operational aspects for the main survey phase (switch off due to bright sources, "CalClosed" and/or "Closed" filter during passage of bright X-ray and/or optical sources, etc). Especially scans close ($\leq 3°$) to Sco X-1 would help to verify the performance of the X-ray baffle.

Details on each target will be provided in a separate document and on the WWW pages.

5.5 Targets for performance verification

It is proposed that for performance verification (PV) each Working Group provides a list of suited targets and/or black-listed targets. The PV phase will be covered in detail in a separate document. Data right details for PV phase have to be clarified (default is general survey policy). A few candidate targets are listed in the table below.

Target	RA(2000)	DEC(2000)	Type	GalLon	EclLat
Commissioning:					
LMC (30 Dor)	05 38 42.4	-69 01 02	always visible	279.368	-86.827
Plate scale and boresight of the 7 modules:					
Hyades	04 31 60.00	+18 10 00.0	open cluster	178.972	-3.691
Pleiades	03 47 00.00	+24 07 00.0	open cluster	166.572	4.086
NGC 2516	07 58 20.00	-60 52 13.0	open cluster	273.940	-75.890
NGC 6475	17 53 30.00	-34 49 12.0	open cluster	355.802	-11.388
NGC 752	01 57 41.00	+37 47 06.0	open cluster	137.126	24.061
Gain and CTI:					
1ES 0102-72	01 04 02.00	-72 01 55.0	SNR	301.558	-65.036
LHA 120-N 132D	05 25 15.23	-69 38 12.8	SNR	280.295	-85.540
Vela SNR	08 48 45.75	-45 36 51.4	SNR	265.347	-59.522
Puppis A	08 22 00	-42 55 00	SNR		
3C58	02 05 38.00	64 49 26.0	SNR	130.722	47.914
SNR G021.5-00.9	18 33 33.57	-10 34 07.5	SNR/pulsar	21.502	12.625
Filter integrity (launch and micrometeorites):					
omega Cen (NGC 5139)	13 26 47.24	-47 28 46.5	GC d=10' V=3.7	309.103	-35.228
M4 (NGC 6121)	16 23 35.22	-26 31 32.7	GC d=8.5' V=5.6	350.974	-4.869
M22 (NGC 6656)	18 36 23.94	-23 54 17.1	GC d=6.5' V=5.1	9.893	-0.728
47 Tuc (NGC 104)	00 24 05.67	-72 04 52.6	GC d=6' V=4	305.896	-62.353
NGC 6752	19 10 52.11	-59 59 04.4	GC d=3.8' V=5.4	336.494	-37.221
M5 (NGC 5904)	15 18 33.22	+02 04 51.7	GC d=3.5' V=5.7	3.860	19.646
M71 (NGC 6838)	19 53 46.49	+18 46 45.1	GC d=3.3' V=8.2	56.747	38.792
M2 (NGC 7089)	21 33 27.02	-00 49 23.7	GC d=2' V=6.5	55.045	14.509
M15 (NGC 7078)	21 29 58.33	+12 10 01.2	GC d=2' V=6.2	65.014	25.475
NGC 1261	03 12 16.21	-55 12 58.4	GC d=1.4' V=8.3	270.540	-67.273
Soft X-ray response and contamination monitoring:					
1RXS J185635.1-375433	18 56 35.11	-37 54 30.5	INS	358.600	-15.033
1RXS J160518.8+324907	16 05 18.9	+32 49 07	INS	52.877	52.238
1RXS J130848.6+212708	13 08 48.7	+21 27 08	INS	338.748	26.426
1RXS J080623.0-412233	08 06 23.0	-41 22 33	INS	257.427	-59.394
1RXS J042003.1-502300	04 20 02.2	-50 22 46	INS	258.136	-69.494
1RXS J214303.7+065419	21 43 03.8	+06 54 20	INS	62.658	19.419
1RXS J072025.1-312554	07 20 24.961	-31 25 50.21	INS:var	244.159	-52.860
XUV response and contamination monitoring:					
HZ 43	13 16 21.853	+29 05 55.38	WD V=12.7	54.108	34.047
GD 153	12 57 02.337	+22 01 56.68	WD V=13.4	317.261	25.785
PG 1658+441	16 59 48.44	+44 01 03.9	WD V=14.6	69.124	66.033
PG 0136+251	01 38 53.02	25 23 22.8	WD V=16	136.246	14.070
CAL 83	05 43 34.5	-68 22 18	XRB	278.564	-87.602
Power-law type spectrum:					
Mkn 421	11 04 27.314	+38 12 31.80	BL Lac	179.832	29.504
PKS 2155-304	21 58 52.065	-30 13 32.12	BL Lac	17.731	-16.771
MS0737.9+7441	07 44 05.1	+74 33 59	BL Lac	140.266	52.117
MS0317.0+1834	03 19 51.789	+18 45 33.84	BL Lac	165.108	0.382
MS0419.3+1943	04 22 18.0	+19 50 54	BL Lac	176.028	-1.670
PKS 0558-504	05 59 47.4	-50 26 51	Sy1	257.963	-73.887
Mkn 3	06 15 36.458	+71 02 15.24	Sy2	143.297	47.624
Effective area and vignetting:					
1ES 0102-72	01 04 02.00	-72 01 55.0	SNR	301.558	-65.036
LHA 120-N 132D	05 25 15.23	-69 38 12.8	SNR	280.295	-85.540
Vela SNR	08 48 45.75	-45 36 51.4	SNR	265.347	-59.522
Puppis A	08 22 00	-42 55 00	SNR		
3C58	02 05 38.00	64 49 26.0	SNR	130.722	47.914
SNR G021.5-00.9	18 33 33.57	-10 34 07.5	SNR/pulsar	21.502	12.625
4U 1722-30	17 27 33.2	-30 48 07	LMXB in GC	356.321	-7.560
Flatfield and vignetting:					
A1795	13 49 00.5	+26 35 07	ClG:clu	33.790	34.994
A2029	15 10 58.7	+05 45 42	ClG:clu	6.506	22.646

A2256	17 03 43.5	+78 43 03	ClG:lar	111.097	77.224
A754	09 08 50.1	-09 38 12	ClG:lar	239.253	-24.834
A2142	15 58 20.00	+27 14 00.3	ClG:lar	44.232	46.457
A3571	13 47 28.9	-32 51 57	ClG:clu	316.318	-20.297
A2052	15 16 45.5	+07 00 01	ClG:clu	9.395	24.245
A2199	16 28 37.0	+39 31 28	ClG:clu	62.898	60.072
A262	01 52 50.4	+36 08 46	ClG:clu		
A3112	03 17 52.4	-44 14 35	ClG:clu	252.953	-58.950
A85	00 41 37.8	-09 20 33	ClG:clu	115.054	-12.700
A780 (Hydra A Cluster)	09 18 10	-12 05 00	ClG:clu	243.138	-26.529
MKW 3s	15 21 50.7	+07 42 18	ClG:clu	11.392	25.278
A2204	16 32 45.7	+05 34 43	ClG:clu	21.091	27.177
A1835	14 01 02.07	+02 52 43.2	ClG:clu	340.386	14.257
A496	04 33 35.00	-13 14 46.0	ClG:clu	209.564	-34.766
A1060	10 36 51.3	-27 31 35	ClG:clu	269.631	-33.312
A3827	22 01 49.1	-59 57 15	ClG:clu	332.227	-44.106
PSF:					
Cen X-3	11 21 15.78	-60 37 22.7	HMXB	292.092	-56.339
Mkn 766	12 18 26.484	+29 48 46.15	Sy1	190.681	28.939
Mkn 205	12 21 44.967	+75 18 37.99	Sy1	125.446	63.773
PKS 0312-770	03 11 55.233	-76 51 50.87	Sy1	293.441	-73.870
3C 273	12 29 06.695	+02 03 08.66	Quasar	289.952	4.774
QSO B0836+71	08 41 24.365	+70 53 42.17	Quasar	143.542	50.150
SMC X-1	01 17 05.146	-73 26 36.03	HMXB	300.416	-66.470
PKS 0558-504	05 59 47.4	-50 26 51	Sy1	257.963	-73.887
PG 1634+706	16 34 28.990	+70 31 32.42	Quasar	102.842	81.295
X-ray baffle (mosaic or mini-survey):					
Sco X-1 (offset)	16 19 55.00	-15 38 24.0	LMXB	359.095	5.725
Crab (offset)	05 34 31.938	+22 00 52.18	Pulsar+SNR	184.558	-1.294
LMC X-2 (offset)	05 20 28.04	-71 57 53.3	LMXB	283.100	-83.579
LMC X-3 (offset)	05 38 56.299	-64 05 03.00	HMXB	273.577	-86.691
Masked mode:					
GX 13+1	18 14 31.55	-17 09 26.7	LMXB	13.517	6.238
GX 17+2	18 16 01.389	-14 02 10.62	LMXB	16.433	9.348
Timing:					
PSR B0540-69	05 40 11.221	-69 19 54.98	50ms	279.718	-86.665
PSR B1929+10	19 32 13.950	+10 59 32.42	226ms	47.383	32.291
PSR J1210-5226	12 10 00.91	-52 26 28.4	424ms	296.546	-45.784
Cen X-3	11 21 15.78	-60 37 22.7	4.84s	292.092	-56.339
1E 1048.1-5937	10 50 08.93	-59 53 19.9	6.4s	288.261	-58.601
PSR J1930+1852	19 30 30.13	+18 52 14.1	136ms	54.097	40.104
PSR J1119-6127	11 19 14.30	-61 27 49.5	408ms	292.152	-57.102
Miscellaneous:					
3C 382	18 35 03.390	+32 41 46.86	Sy1	61.306	55.736
Ark 564	22 42 39.309	+29 43 31.55	Sy1	92.139	34.702
1H 1426+428	14 28 32.600	+42 40 21.08	BL Lac	260.170	-70.866
Performance verification:					
zeta Ori field offset	05 40 45.00	-01 56 30.0		206.451	-25.292
WW Hor	02 36 12.00	-52 19 12.0	CV: AM Her	272.227	-61.559
Tycho	00 25 22.00	+64 08 24.0		120.094	53.750
M31	00 42 43.00	+41 16 12.0	diffuse+point	121.171	33.352
NGC 253	00 47 34.00	-25 17 24.0	soft diffuse	97.435	-27.779
A 189	01 25 25.00	+01 44 28.0		140.105	-6.713
Virgo M87	12 30 50.00	+12 23 24.0		283.789	14.417
Coma Cluster	12 59 46.7	+27 57 00		57.378	31.375
Perseus Cluster	03 19 47.2	+41 30 47		150.573	22.340
Cygnus Loop SW	20 49 00	+30 15 00		73.381	45.771
Galactic Center Sgr A*	17 45 40.041	-29 00 28.12		359.945	-5.608

5.6 References for target classes and objects

- "Cross-calibrating X-ray detectors with clusters of galaxies: an IACHEC study", J. Nevalainen, L. David, M. Guainazzi, A&A 523, A22 (2010), doi: 10.1051/0004-6361/201015176
- "Cross-calibration of the X-ray instruments onboard the Chandra, INTEGRAL, RXTE, Suzaku, Swift, and XMM-Newton observatories using G21.5-0.9" M. Tsujimoto, M. Guainazzi, P.P. Plucinsky, A.P. Beardmore, M. Ishida, L. Natalucci, J.L.L. Posson-Brown, A.M. Read, R.D. Saxton, N.V. Shaposhnikov, A&A 525, A25 (2011), doi: 10.1051/0004-6361/201015597
- "Cross-calibration of the x-ray instruments onboard the Chandra, Suzaku, Swift, and XMM-Newton Observatories using the SNR 1E 0102.2-7219", P.P. Plucinsky, A.P. Beardmore, J.M. DePasquale, D. Dewey, A. Foster, F. Haberl, E.D. Miller, A.M.T. Pollock, J.L.L. Posson-Brown, S. Sembay, R.K. Smith, Proc. SPIE 8443, 844312 (2012), doi: 10.1117/12.926506
- "Cross Spectral Calibration of Suzaku, XMM-Newton, and Chandra with PKS 2155-304 as an Activity of IACHEC", M. Ishida, M. Tsujimoto, T. Kohmura, M. Stuhlinger, M. Smith, H.L. Marshall, M. Guainazzi, K. Kawai, T. Ogawa, PASJ 63, S657 (2011)
- "Establishing HZ43 A, Sirius B, and RX J185635-3754 as soft X-ray standards: a cross-calibration between the Chandra LETG+HRC-S, the EUVE spectrometer, and the ROSAT PSPC", K. Beuermann, V. Burwitz, T. Rauch, A&A 458, 541 (2006), doi: 10.1051/0004-6361:20065478